



Potential anticancer activity and staining of tissue by new azo pyridyl dye and its palladium complex

Dhifaf Abdulhadi Al-Asadi¹, Hasan Shamran Mohammed^{1,2,*}¹Chemistry department, Science college, University of Al-Qadisiyah, Iraq²Laboratory of Advanced Materials and Physicochemistry for Environment and Health, Djillali Liabes University of Sidi Bel Abbas, Algeria

ARTICLE INFO

Article history:

Received 13 July 2024

Received in revised form 20 August 2024

Accepted 26 August 2024

Available online 20 September 2024

Keywords:

Stain,
MTT,
pyridyl,
palladium,
azo.

ABSTRACT

Heterocyclic azo dye namely methyl (E)-4-hydroxy-3-(pyridin-3-yl)diazonylbenzoate (MHPDB) has been synthesized from 3-aminopyridine which serves as the diazonium salt and coupling with methyl 4-hydroxybenzoate component to form the dye. The palladium complex was synthesized by reacting two equivalent of MHPDB ligand with an equivalent of palladium chloride. The synthesized compounds were characterized by H-NMR, IR, UV-Vis spectroscopies and elemental analysis. The MHPDB ligand is bidentate based on infrared data and the palladium complex is square planer. The UV-Vis spectral demonstrate that the heterocyclic dye MHPDB shows red shift in basic medium comparison with the acidic medium where the backbone of dye owing better electron delocalization for heterocyclic system in basic medium. The synthesized compounds exhibited potential anticancer activity against A375 cell line. The IC₅₀ of palladium complex was 66.44 µg/mL against A375 cell line while its IC₅₀ was 137.0 µg/mL against HdFn health cell. The synthesized commands showed very good staining for ovary, uterus and intestine in mice.

1. Introduction

Synthetic heterocyclic compounds have demonstrated excellent against different diseases especially pyridine compounds and the derivatives of azo moiety which have shown tremendous potential against antimicrobial, antiviral, antidiabetic, anti-melanogenic, anti-ulcer, anti-mycobacterial, anti-inflammatory, DNA binding and chemosensing activities [1].

The heterocyclic compounds of pyridine derivatives and phenols showed demonstrated remarkable promise against different diseases and exhibited plenty of applications. On the other hand, the incorporation of a diazo group is crucial for the improved efficacies of these compounds in probing different diseases [2–4]. Number of diazenyl compounds and diazenyl complexes showed cytotoxic potential in the direction of various cancer cell lines by interacting with various receptors or enzymes which cause DNA damage, necrosis or apoptosis which lead to cell death [5, 6]. Molecular antennas based on pyridine copper(I) and azo dyes showed attention behaviour to be

used in the formation of very efficient solar systems utilising DSSC technology [7–9]. Incorporation of azo chromophores with dopamine using biscatecholic colorants showed efficiency to colour various textiles [10, 11]. Therefore, we are interested in preparing azo ligand of pyridyl and its palladium complexes and study of their potential activity as anticancer compounds and their ability in staining the tissues.

2. Computational details

We used devices of Stuart digital melting point/SMP3, Uv-1650 PCUV-Visible spectrophotometer, Infrared Spectrophotometer Shimadzu, Agilent Technologies 5973C Bestic Germany Aluminum, Bruker 400 MHZ Spec, Philips PW 9421 pH meter.

The materials supplied from different companies. 3-Amino Pyridine and Palladium (II) Chloride from Sigma-Aldrich, 4-Hydroxy Methyl Benzoate from MERCK, Dimethyl Sulfoxide (DMSO), Sodium hydroxide and Sodium nitrite from B.D.H, Ethanol absolute and Hydrochloric acid from Scharlu,

* Corresponding author; e-mail: hasan.sh.mohammed@qu.edu.iq<https://doi.org/10.22034/crl.2024.467690.1379>

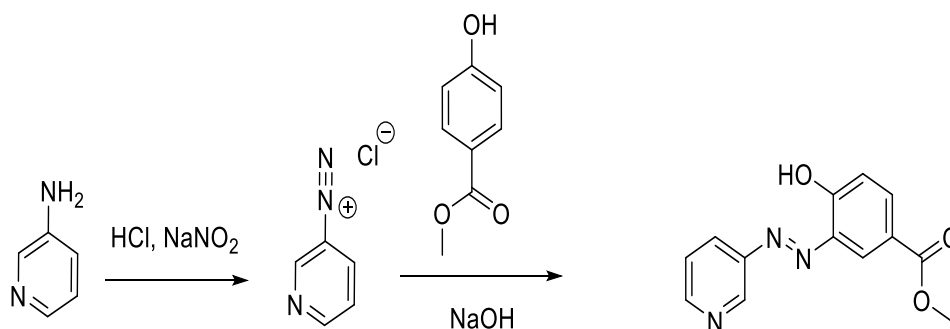
This work is licensed under Creative Commons license CC-BY 4.0

2.1 Preparation of MHPDB ligand of 3-aminopyridine

3-aminopyridine 0.5 g of 0.005 mol was dissolving in 15 mL of distilled water, then it was mixed with 3 mL of concentrated hydrochloric acid (HCl, 37%) and then the solution was cooled at 0-5 C. Sodium nitrite NaNO₂ (0.36 g, 0.005 mole) was dissolved in 5 ml of distilled water and then the solution was put under cooling the solution to 0 0. The cold solution of sodium nitrite was added to the acidic solution of 3-aminopyridine to form diazonium salt.

The diazonium salt solution was added drop by drop with continuous stirring under cooling to the coupling compound solution of 4-hydroxy methyl benzoate 0.77 g, 0.005 mol dissolving in 10 ml of ethyl alcohol containing 10 ml of 10% sodium hydroxide solution. The solution was left to settle for 30 minutes. Then it was left until the second day. The precipitate was filtered and then washed with distilled water and ethyl alcohol. The ligand was a light orange powder. Yield: 85 %. Elemental analysis: of C₁₃H₁₁N₃O₃, Theo C, 60.70; H, 4.31; N, 16.33%. Found C, 60.43; H, 4.12; N, 16.56 %.

2.2 Preparation of palladium complex [Pd(MHPDB)₂]



Scheme 1. Preparation steps of MHPDB of 3-aminopyridine.

3.1 pH effect on spectral properties of MHPDB ligand

UV-Vis spectroscopic technique was chosen for the stimulating pH-controlled absorption behaviour of ligand as chemosensor. The assessment of pH effect on the MHPDB ligand at 10⁻⁴ molar indicates to a dramatically red-shifted from 380 nm in the acidic medium to 473 nm in the basic medium and the color turns from yellow to dark red as shown in Figure 1. That means that, there is π -conjugated system of the diazo component more than in the neutral medium which the maximum absorption wavelength was 445 nm and the color was orange [13].

The synthesized dye MHPDB has high sensitivity in pH range from 2- 10 and could be applied as a selective 'naked-eye' colorimetric sensor for H ion

The MHPDB ligand (0.002 mole, 0.52 g) was dissolved in 10 ml of ethanol and was mixed with 0.05 g, 0.002 mole of sodium hydroxide for deprotonation the ligand. Palladium chloride (0.001 mole, 0.17 g) was dissolved in 15 mL of distilled water with two drops of hydrochloric acid, and the solution was stirring for 30 minutes for completing the solubility. The ligand solution was added on the palladium chloride solution and the acidity of the mixture reaction solution was adjusted at pH=8. The mixture solution was refluxed for 2 hours. We noticed the formation of a dark brown precipitate. The precipitate was filtered and was washed several times with distilled water and then allowed to dry. The complex was a dark brown powder. Yield: 76 %. Elemental analysis: of C₂₆H₂₀N₆O₆Pd. Theo C, 50.46; H, 3.26; N, 13.58%. Found C, 50.15; H, 3.27; N, 13.51 %.

3. Results and Discussion

To improve the bioactive properties of the azo dye target derivatives, we incorporated heterocyclic moiety of pyridyl into the azo dye [12]. The MHPDB ligand was prepared from the reaction of diazonium salt of 3-aminopyridine with the compound of methyl 4-hydroxybenzoate. The MHPDB ligand was precipitated in a neutral to slightly basic medium according to Scheme 1.

concentration, which exhibited a very strong hyperchromic shift in the absorption band from 387-473 nm with a significant color change from yellow to red. The sensitivity of chemosensor was observed to be fully reversible and rapid. That leads to use the dye as a selective "naked-eye" colorimetric sensor for H ion concentration and indicator in titration of acid-base reactions [14–16].

Solid metal complex of divalent palladium metal for 3-[3-pyridylazo]-methyl-4-hydroxybenzoate (MHPDB) was prepared by mixing 0.001 mole of hot palladium chloride solution with 0.002 mole of MHPDB ligand mixing with two equivalents of sodium hydroxide as shown in Scheme 2. The mixture of reaction was refluxed for an hour observing the color change. The solution was left overnight then it was filtration.

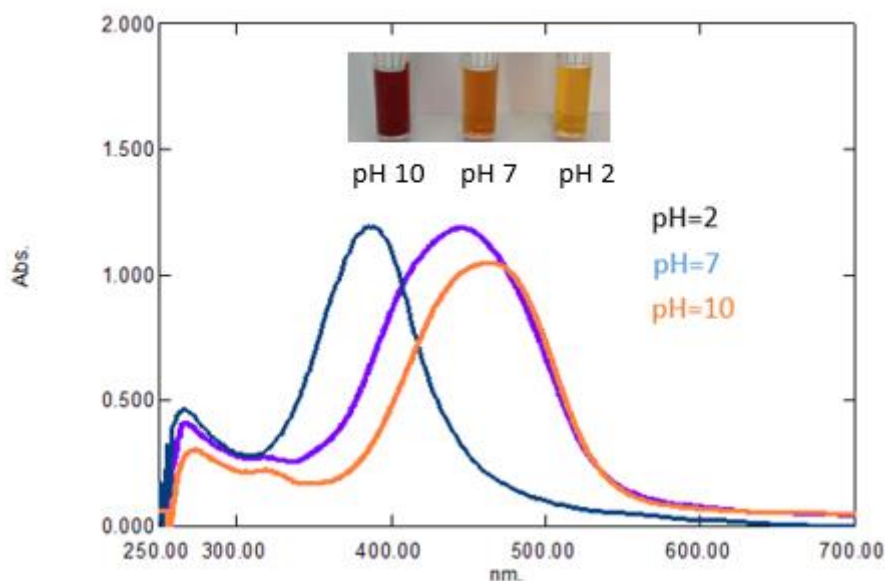
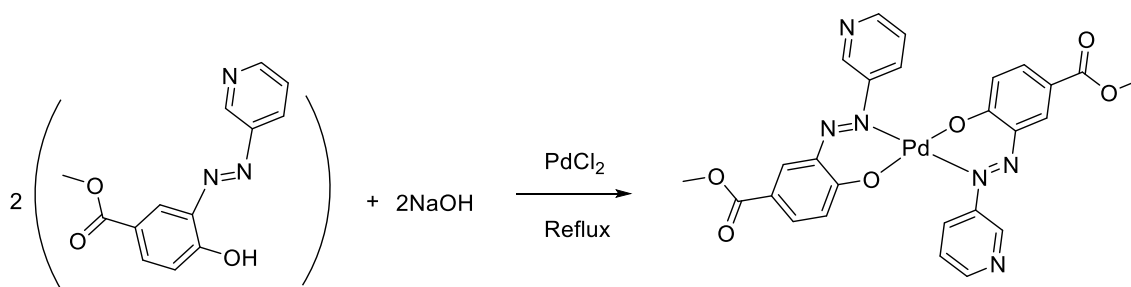


Fig. 1. Effect of pH on the electronic spectra of the MHPDB ligand.



Scheme 2. Preparation steps of palladium complex for MHPDB ligand.

The MHPDB ligand and its palladium complex were identified, through precise quantitative analysis of the elements (C.H.N.), and by matching the results calculated theoretically and the results obtained practically. The mass (m/z) of MHPDB ligand as shown in Figure 2, was 257.2 and the mass of palladium complex was 618.9 which are in agreement with suggest formulas. The molar conductivity of the palladium complex in the dimethyl sulphur dioxide solvent was conducted at room temperature to determine the ionic nature of the complex at a concentration of (10^{-3} M). The conductivity value was $5.2 \Omega^{-1} \cdot \text{cm}^2 \cdot \text{mol}^{-1}$, which indicates that the palladium complex with the MHPDB ligand has a non-ionic nature.

3.2 Proton NMR spectra of MHPDB ligand and its palladium complex

The structure of MHPDB ligand and palladium complex were confirmed by $^1\text{H-NMR}$ spectroscopic as shown in Figures 3 and 4 respectively, which were done in deuterated dimethylsulphoxide (DMSO d_6) solvent.

In the $^1\text{H-NMR}$ spectrum of MHPDB ligand, the singlet signal at 9.24 ppm indicated to the presence of hydroxyl OH group in the structure of the ligand. The aromatic protons were present in the range of 7.22 to 8.82 ppm. The protons beside the azomethine group ($\text{C}=\text{N}$) appeared in low field as a singlet signal at 8.76 ppm and doublet signal at 8.38 ppm which are due for the reacting of azomethine group ($\text{C}=\text{N}$) as withdrawing group which increases the deshielding on these protons [17]. The methyl protons of methoxy group appeared at 3.79 ppm because of deshielding reacting by oxygen atom of methoxy group. The chemical shift at $\text{ppm} = 2.5 \delta$ returns to the solvent (DMSO- d_6) and a signal showed at 3.34 ppm due to residual water in DMSO solvent.

The palladium complex showed similar H-NMR spectrum for the MHPDB ligand excepting the proton of OH disappearing. The aromatic protons showed in the range of 6.97-8.74 ppm. The protons besides azo group on phenol ring and pyridine ring appeared in higher filed than in MHPDB ligand. These indicators give evidence to form the complex and the number of signals refers to symmetry of MHPDB ligands on palladium metal.

File :C:\MSDCHEM\1\DATA\Snapshot\DAS2 .D
 Operator :
 Acquired : 24 Apr 2023 17:38 using AcqMethod default.m
 Instrument : direct mass
 Sample Name:
 Misc Info :
 Vial Number: 1

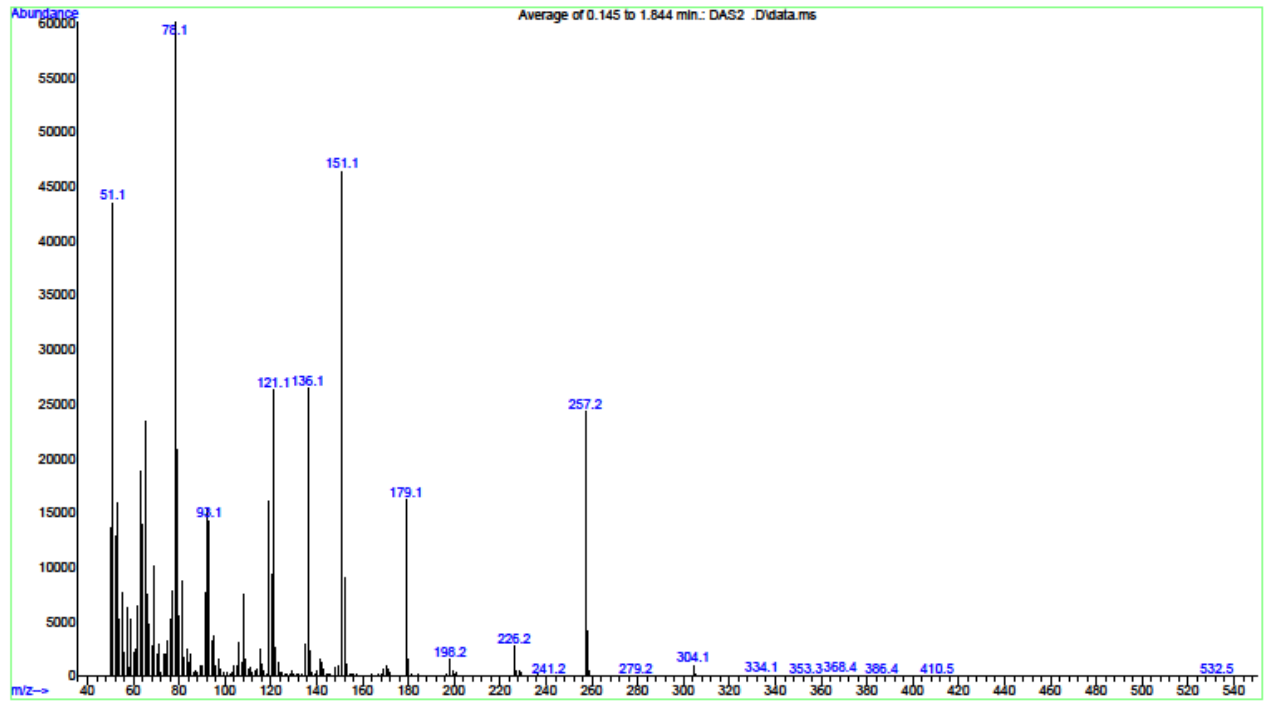


Fig. 2. Mass spectrum of MHPDB ligand.

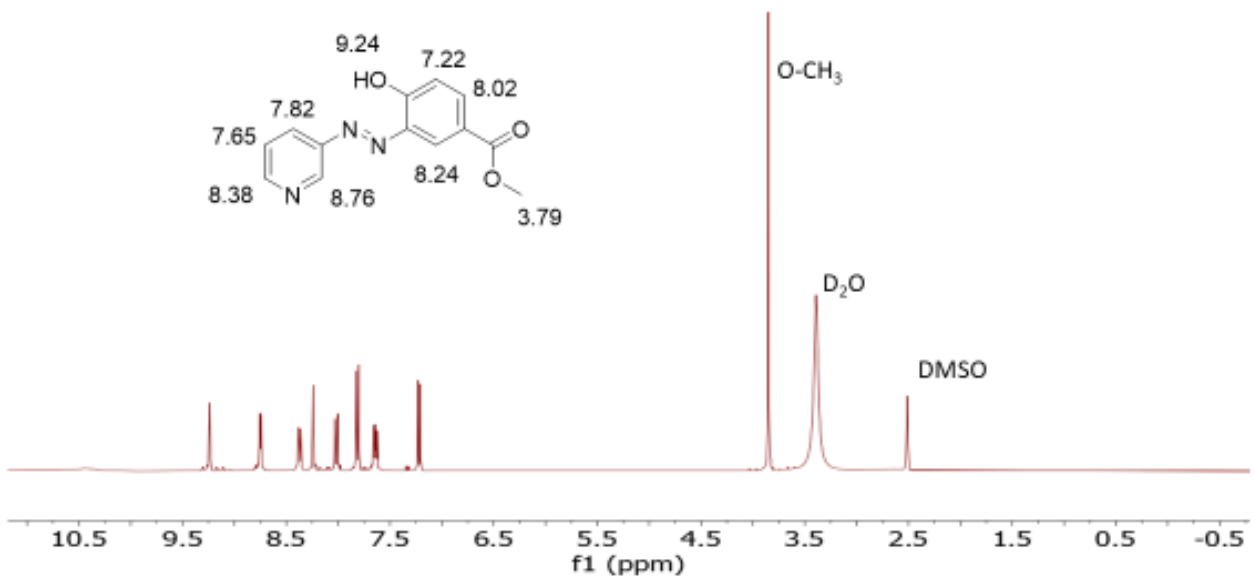


Fig. 3. ¹H-NMR spectrum of MHPDB ligand.

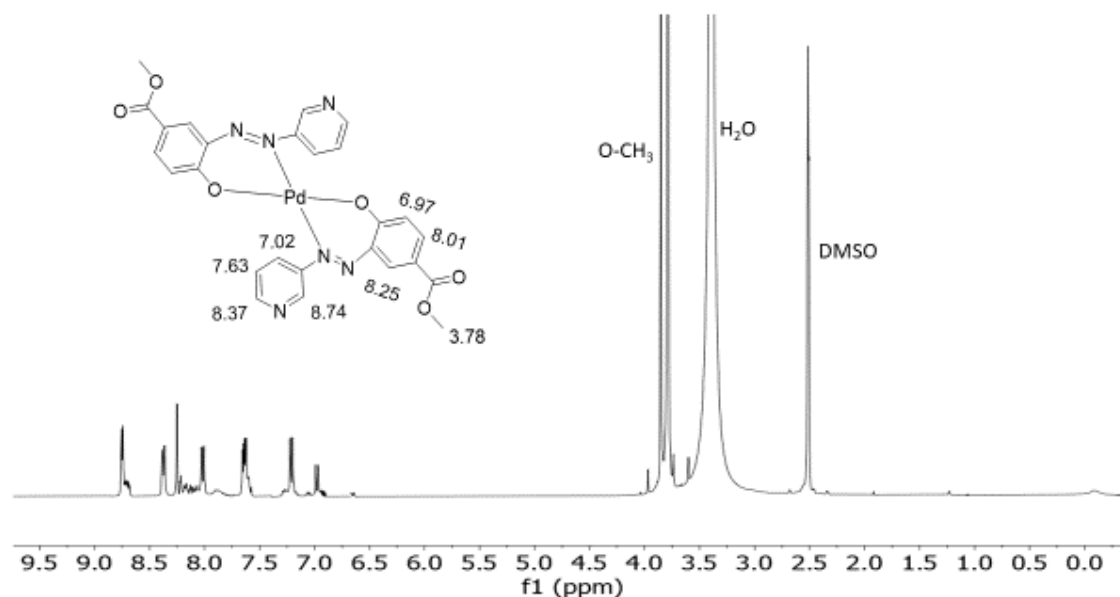


Fig. 4. $^1\text{H-NMR}$ spectrum of palladium complex of MHPDB ligand.

3.3 Infrared spectra of MHPDB ligand and its palladium complex

Infrared spectroscopy is an important technique to characterize active groups in compounds. The MHPDB ligand showed many characterization peaks. The O-H group is an important group that appeared at 3357 cm^{-1} in a strong and sharp in the spectrum of the ligand as shown in Figure 5, which disappeared in the spectrum of palladium complex as shown in Figure 6 [18]. In addition, other groups such as CH of the aromatic and aliphatic, and the C=O groups appeared at 3046 , 2956 , 1683 cm^{-1} respectively. The C=C groups appeared at 1585 and 1513 cm^{-1} . In-plane bending of CH aromatic appeared at 1027 cm^{-1} and the out-of-plane bending CH

at 828 cm^{-1} , as well as the Ar-O group appeared at 1352 cm^{-1} , which in turn suffered a change after coordination of the MHPDB ligand to the palladium metal ion to be 1282 cm^{-1} . The ligand (MHPBD) also showed absorption at 1464 cm^{-1} due to the N=N group, which suffered a change in location and intensity in the spectrum of the palladium complex. That indicates to coordinate nitrogen atom with the palladium metal ions in the complex. The absorption of C=O and C=N did not appear a change in location or intensity in the spectrum of palladium complex, which indicate these functional groups did not participate in coordination with the palladium ions. New bands appeared at low frequencies at 418 and 640 cm^{-1} , due to M-O and M-N absorptions respectively.

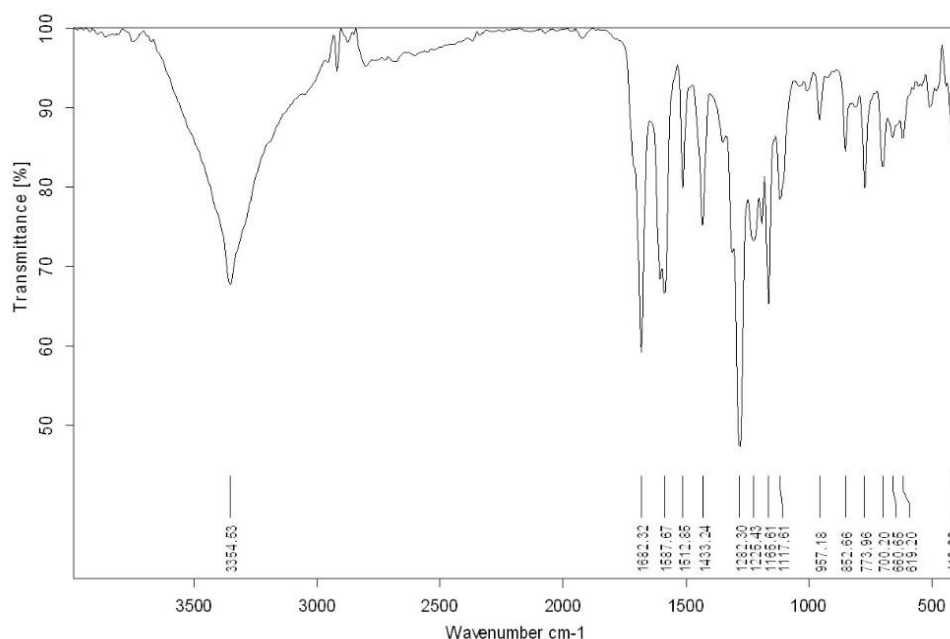


Fig. 5. Infrared spectrum of MHPDB in KBr pellet.

3.4 Electronic transitions of MHPDB ligand and its palladium complex

The UV-Vis spectrum of the MHPDB showed three electronic transitions in the DMSO solvent at laboratory temperature as shown in Figure 7. The first and second electronic transitions at 271 nm and 312 nm respectively, are attributed to the electronic transition of $\pi \rightarrow \pi^*$ transitions. The third band appeared at a wavelength of 420 nm, which is attributed to the $n \rightarrow \pi^*$ electronic transition [19].

The UV-Vis spectrum of the palladium complex showed several transitions at (295 nm) and 381 nm due to azo ligand's transitions. The electronic transitions at (537 nm) and (620 nm) are attributed to electronic transitions of the type ($^1A_{2g} \rightarrow ^1T_{1g}$) and ($^1A_{1g} \rightarrow ^1B_{1g}$) respectively with the diamagnetic properties of the palladium(II) complex, these results and diamagnetic properties are consistent with the planar palladium complexes [20, 21].

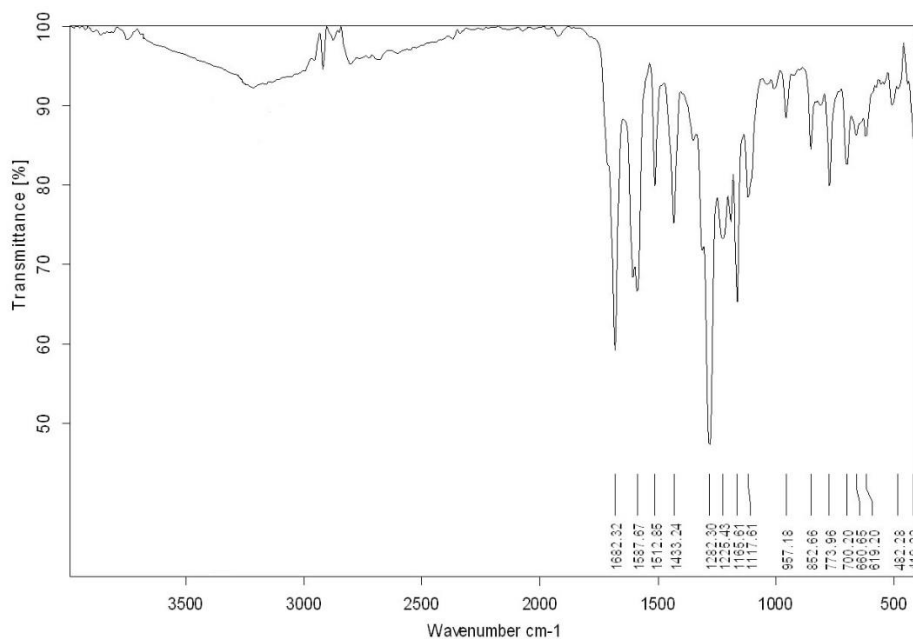


Fig. 6. Infrared spectrum of palladium complex for MHPDB ligand.

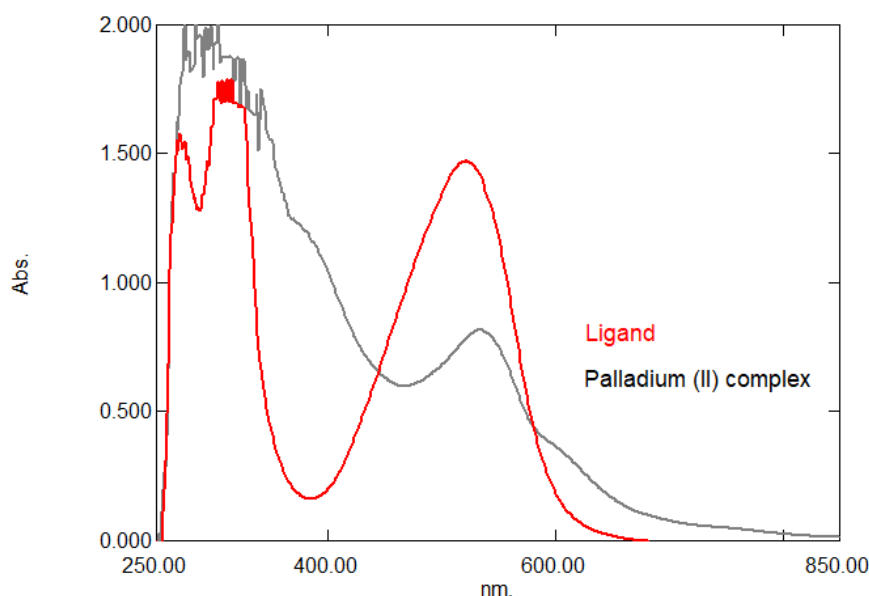


Fig. 7. UV-Vis spectra of MHPDB ligand and its palladium complex.

3.5 X-ray diffraction measurements of MHPDB ligand and its palladium complex

The crystal structure of MHPDB ligand and its palladium complex was studied using X-rays within the

angular range ($^{\circ} 90-0$) 2θ , where the total width at half the maximum height, the angle of deviation, and the crystal size were calculated using the Debye-Scherrer equation. The XRD patterns of MHPDB ligand and its

palladium complex are shown in Figures 8 and 9. The XRD data of the MHPDB ligand and its palladium (II) complex are depicted in Tables 1 and 2. The XRD data and sharp peaks of the synthesized compounds refer to crystalline structure for them and in the range of nanomaterial depending on crystal size. The higher intensity peaks of MHPDB ligand were observed in the

palladium complex indicating that the palladium ion is incorporated within the MHPDB ligand environment. The azo ligand and its palladium complex showed crystalline structure with sharp peaks but the palladium complex is more crystalline because of its sharper peaks and lower full width half maximum (FWHM) values.

Table 1. XRD data for MHPDB ligand.

Pos. [$^{\circ}2\theta$.]	Height [cts]	FWHM Left [$^{\circ}2\theta$.]	d-spacing	Crystal seize [nm]
12/5016	131/56	0/1968	7/08054	42.43
12/9024	154/95	0/3149	6/86152	26.53
17/0389	116/96	0/3149	5/20392	26.65
17/9683	287/78	0/2755	4/93679	30.50
18/4929	338/03	0/3149	4/79792	26.71
19/3334	206/62	0/1968	4/59120	42.79
24/9620	680/26	0/2755	3/56724	30.86
25/7377	309/58	0/2755	3/46146	30.91
26/6326	346/32	0/5510	3/34714	15.48
27/7462	151/49	0/3936	3/21529	21.72
31/7609	612/63	0/0984	2/81744	87.70
45/5670	176/23	0/2362	1/99080	38.12

Table 2. XRD data of Pd(II) complex.

Pos. [$^{\circ}2\theta$.]	Height [cts]	FWHM Left [$^{\circ}2\theta$.]	d-spacing	Crystal seize [nm]
18/7218	173/44	0/1574	4/73978	53.45
25/3828	176/77	0/1181	3/50904	72.05
26/4991	427/65	0/1378	3/36370	61.88
31/8703	2170/71	0/0984	2/80801	87.73
40/1055	171/74	0/9446	2/24838	9.35
45/5307	504/66	0/0787	1/99230	114.39
66/2854	430/48	0/1200	1/40893	82.62
66/4880	190/18	0/0960	1/40862	103.40
75/3292	202/10	0/1440	1/26064	72.83
84/0480	110/63	0/1200	1/15066	93.14

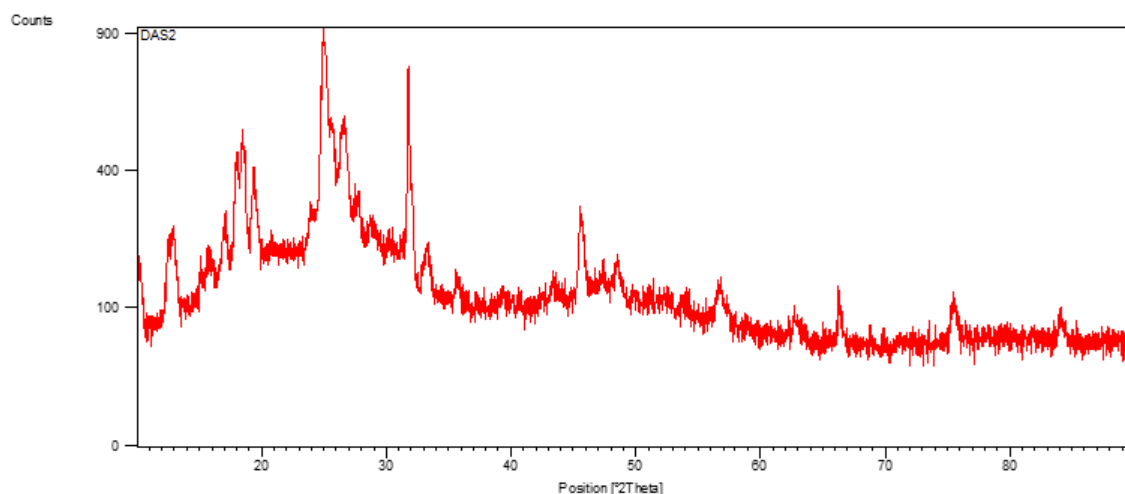


Fig. 8. Pattern of XRD Powder of MHPDB ligand.

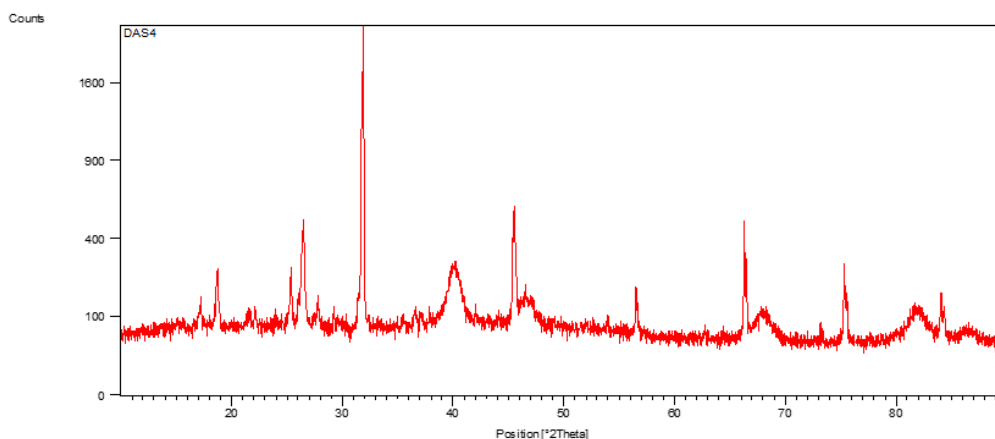


Fig. 9. Pattern of XRD Powder of palladium complex for MHPDB ligand.

3.6 Anticancer activity by MTT

Significant apoptotic in cancer cells can be induced by cisplatin especially in the treatment case for melanoma [22, 23]. The treatment by cisplatin showed many well-known limitation effects such as tumor resistance to medications and cytotoxicity such as ototoxicity, nephrotoxicity, and leukopenia, therefore we are interested in using new compounds [23-25]. The prepared compounds have done their anticancer activity in human tumor cell lines for A375. The A375 is cell line showing an epithelioid morphology which was isolated from the skin of a 54-year-old female patient with malignant melanoma.

The in vitro, MTT data indicated to promising activity against A375 cells by MHPDB ligand and palladium complex. In particular, the MHPDB ligand showed potential activity

against the A375 cells human tumor lines where its IC₅₀ was 100.9 µg/mL for ligand as shown in Figure 10, while its IC₅₀ was 231.9 µg/mL against health human cells of HdFn. The IC₅₀ value is an important parameter in cytotoxicity which indicates to the ligand or complex concentration needing to inhibit a biological process by halve. On the other hand, the palladium complex showed important activity against the A375 cells human tumor where its IC₅₀ was 66.44 µg/mL while its IC₅₀ was 137.0 µg/mL against health human cells of HdFn as shown in Figure 11. Important point, that azo dye of

pyridine and its palladium complex was potent candidate against the A375 human tumor cell lines [26]. From Tables 3, 4, the effect of MHPDB and Pd (II) complex on cancer cells increases with concentration. This behaviour or phenomenon is known as dose dependence.

The cells and tissue are colorless under the light microscope; therefore, we employ staining process to make differential coloration that enables to clearer observation and analysis of cells [27,28]. Swiss albino mice of both sexes (five animals) were sacrificed by cervical dislocation and the intestine, ovary, and uterus were immediately dissected. Figure 12, including images 1-4, showed the histological section of the ovary (1 and 2), uterus, and small intestine (3 and 4) in mice stained with ligand. The azo-ligand showed a strong reaction to the distribution of elastic fibers (blue arrows) and fibroblasts (blue head), brush borders (orange arrow) and panthelial cells (black arrows). 1,2,3 & 4: X400.

Figure 13 represents histological section of the (1,2 & 3) ovary and uterus and (3) small intestine in mice stained with Pd(II) complex. The palladium complex showed moderate reaction stain for elastic fiber distribution(blue arrows, black arrow) and specific stain for RBC (orange arrows and fibroblast (head arrow orange) and basement membrane & brush border (green arrows). 1,2,3& 4: X400.

Table 3. Effect of the MHPDB ligand on the melanoma cancer cell line using the method (MTT) for 24 hours at 37°C.

MHPDB Conc.(µg/mL)	HdFn		A375	
	mean	SD	mean	SD
400	77.27633	3.653575	60.301	2.765341
200	86.034	0.853534	64.85333	1.662477
100	92.12967	1.557424	77.62333	2.411951
50	96.18033	1.251681	90.58667	1.801743
25	96.95233	1.141793	94.79167	1.334742
12.5	94.90733	2.198868	95.40933	1.414488

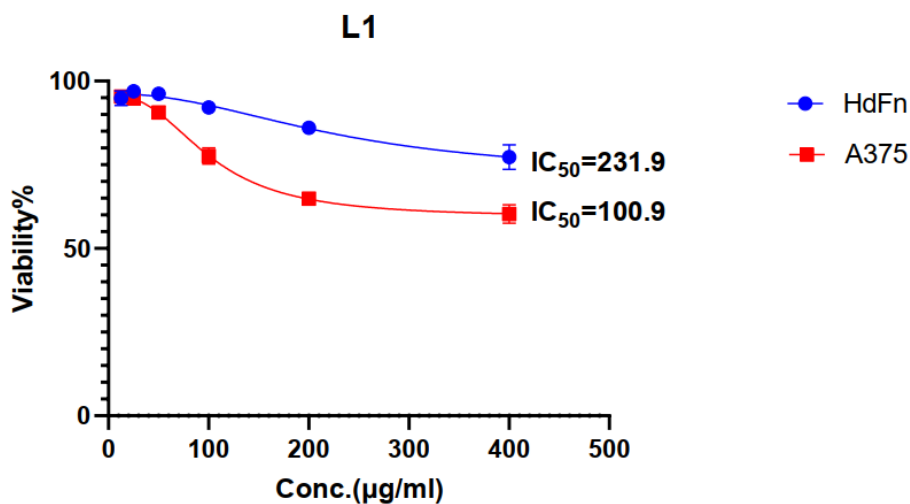


Fig. 10. The relationship between the biological activity of A375 cancer cell lines versus the concentrations of MHPDB ligand.

Table 4. Effect of the palladium complex on the melanoma cancer cell line using the method (MTT) for 24 hours at 37°C.

Pd complex	HdFn		A375	
	mean	SD	mean	SD
Conc. (µg/mL)				
400	69.17467	2.215501	35.648	3.196657
200	73.341	1.075329	41.628	1.621871
100	89.12033	2.323179	53.89667	5.875977
50	93.78867	0.240513	74.344	4.13512
25	94.63767	1.626003	89.429	4.386674
12.5	95.06167	1.646585	95.25467	1.728466

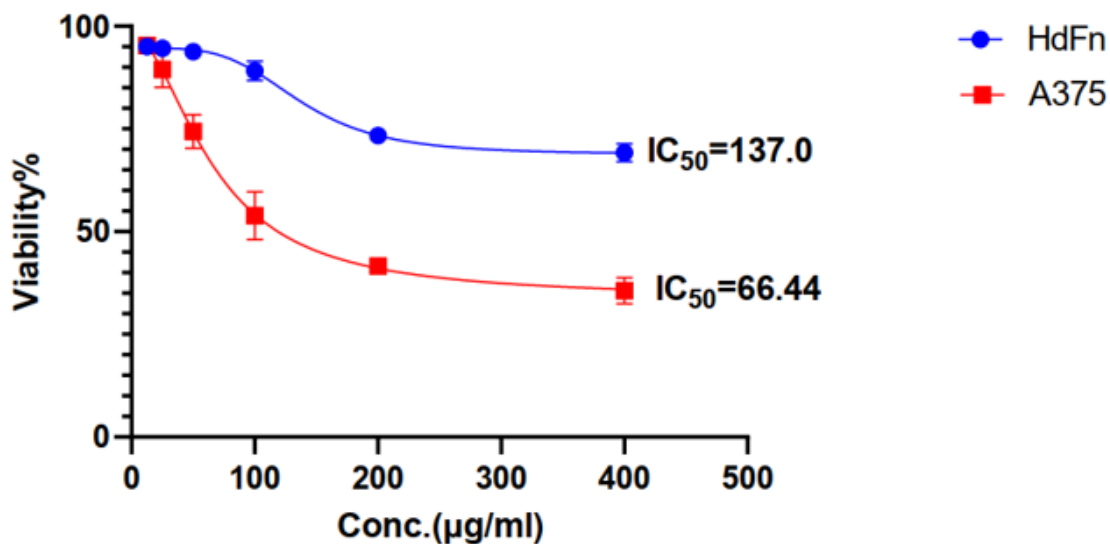


Fig. 11. The relationship between the biological activity of A375 cancer cells versus the concentration of the palladium complex.

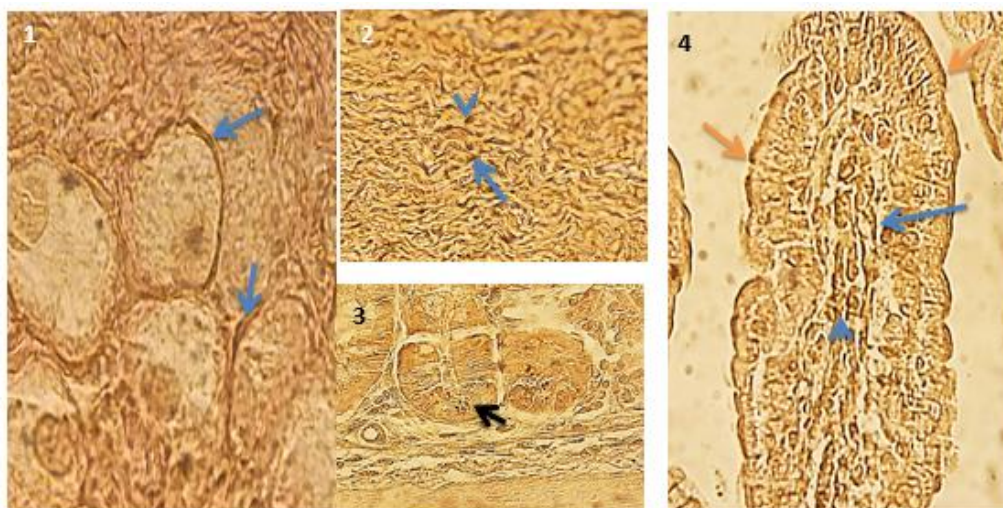


Fig. 12. Histological section of the (1&2) ovary and uterus and (3&4) small intestine in mice stained with azo ligand.

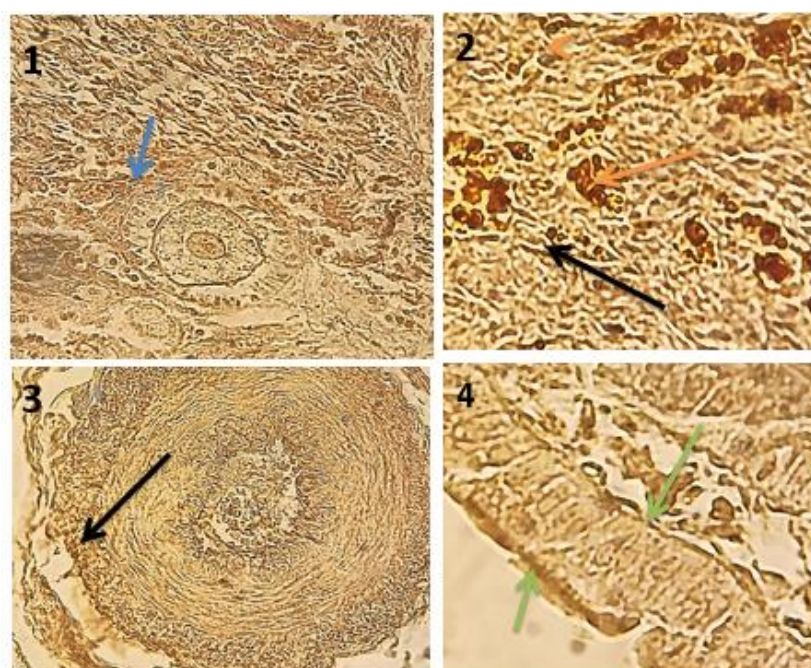


Fig. 13. Histological section of the (1,2&3) ovary and uterus and (4) small intestine in mice stained with Pd(II) complex.

4. Conclusion

Bidentate azo ligand of pyridyl and its palladium complex were synthesized and characterized. The structural characterization of the synthesized compounds has been estimated by Infrared, UV-Vis, H-NMR, powder X-ray diffraction spectroscopies. XRD technique reveals that azo ligand and Pd metal complex are nanoparticle and crystal. The sharp peaks in the XRD patterns of synthesized compounds signify the good crystalline. The synthesized compounds showed potential activity as anticancer compounds and dyes for staining the tissue.

References

- [1] T. Tehreem, M. Ashfaq, M. Saleem, M. Rafiq, M. Shahzad, K. Kotwica-Mojzych, and M. Mojzych, Pyridine scaffolds, phenols and derivatives of azo moiety: current therapeutic perspectives. *Mol.*, 26 (2021) 4872.
- [2] M. Sheydaei; M. Edraki, Antimicrobial evaluation of *Garcinia cambogia*-impregnated sodium montmorillonite, *Chem. Res. Technol.* 1 (2024) 16-21.
- [3] M. Marinescu, C. Popa, Pyridine Compounds with Antimicrobial and Antiviral Activities, *Int. J. Mol. Sci.*, 23 (2022) 5659-5670.
- [4] H. Mohammed, Synthesis, characterization, structure determination from powder X-ray diffraction data, and biological activity of azo dye of 3-aminopyridine and its complexes of Ni (II) and Cu (II). *Bull. Chem. Soc. Ethiop.*, 34 (2020) 523–532.
- [5] N. Shajari, R. Ghiasi, A. Ramazani, Experimental and computational insights for identification of dialkyl 5-oxo-5H-[1,3]thiazolo[3,2-a]pyrimidine-2,3-dicarboxylates, *Chem. Rev. Lett.* 6 (2023) 24-28. 10.22034/crl.2023.371365.1192

- [6] A. Abdou, H. Mostafa, and A. Abdel-Mawgoud, Seven metal-based bi-dentate NO azocoumarine complexes: Synthesis, physicochemical properties, DFT calculations, drug-likeness, in vitro antimicrobial screening and molecular docking analysis. *Inorganica Chim. Acta*, 539 (2022) 121043.
- [7] A. Peppas, D. Sokalis, D. Perganti, G. Schnakenburg, P. Falaras, and A. I. Philippopoulos, Sterically demanding pyridine-quinoline anchoring ligands as building blocks for copper(I)-based dye-sensitized solar cell (DSSC) complexes. *Dalton Trans.*, 51 (2022) 15049–15066.
- [8] N. A. Salman, A. Adhab, H. Bahair, M. Sami, R. sadeghzadeh, Oxidative Decarboxylation of Arylacetic Acids: Novel Approach to the Synthesis of Aryl Aldehydes and Ketones, *Chem. Rev. Lett.* 6 (2023) 139-149.
- [9] S. Liu, V. Biju, Y. Qi, W. Chen, and Z. Liu, Recent progress in the development of high-efficiency inverted perovskite solar cells. *NPG Asia Mater.*, 15 (2023) 1-28.
- [10] S. Fan, Y. Lam, L. He, J. Xin, Novel and Sustainable Colorants Developed via Incorporating Azo Chromophores into Dopamine Molecules. *ACS omega*. 23 (2022) 11082-11091.
- [11] S. Nicolai, T. Tralau, A. Luch, and R. Pirow, A scientific review of colorful textiles. *J. Consum. Prot. Food Saf.*, 16 (2021) 5–17.
- [12] K. Mezgebe and E. Mulugeta, Synthesis and pharmacological activities of azo dye derivatives incorporating heterocyclic scaffolds: a review. *RSC Adv.*, 12 (2022) 25932–25946.
- [13] X. Zhao, J. Geng, H. Qian, and W. Huang, pH-induced azo-keto and azo-enol tautomerism for 6-(3-methoxypropylamino)pyridin-2-one based thiophene azo dyes, *Dyes Pigment.*, 147 (2017) 318–326.
- [14] S. Qamar, Z. Akhter, S. Yousuf, and F. Perveen, pH-sensitive 4,(4-Nitrophenoxy)benzeneamine derived azo dye: X-ray crystallographic, DFT and electrochemical studies. *J. Mol. Struct.*, 1220, (2020) 128667.
- [15] H. Mohammed, H. Al-Hasan, Z. Chaieb, Z. Zizi, and H. Abed, Synthesis, characterization, DFT calculations and biological evaluation of azo dye ligand containing 1, 3-dimethylxanthine and its Co (II), Cu (II) and Zn (II) complexes. *Bull. Chem. Soc. Ethiop.*, 37 (2023) 347–356.
- [16] H. Mohammed, Synthesis and Characterization of Some Complexes of Azo-Chalcone Ligand and Assessment of their Biological Activity. *Mater. Plast.*, 58, (2021) 23–31.
- [17] M. Tassé, H. Mohammed, C. Sabourdy, S. Mallet-Ladeira, P. Lacroix, and I. Malfant, Synthesis, crystal structure, spectroscopic, and photoreactive properties of a ruthenium(II)-mononitrosyl complex. *Polyhedron*, 119 (2016) 350–358.
- [18] H. Mubark, I. Witwit, and A. Ali, Synthesis of new azo imidazole ligand and fabricating it's chelate complexes with some metallic ions. *J. Phys. Conf. Ser.*, 1660,(2020) 012031.
- [19] A. Malekhoseini, M. Montazerzohori, R. Naghiha, E. Kokhdan, S. Joohari, Antimicrobial/antioxidant and cytotoxicity activities of some new mercury (II) complexes. *Chemical Review and Letters*, 6 (2023) 166-182.
- [20] A. Abdulrazzaq and A. Al-Hamdani, Synthesis, Characterization, Thermal Analysis Study and Antioxidant Activity for Some Metal Ions Cr (III), Fe (III), Mn (II) and Pd (II) Complexes with Azo Dye Derived from p-methyl-2-hydroxybenzaldehyde. *Baghdad Sci. J.*, 21 (2024) 1960-1960.
- [21] M. Abdulridha, A. Al Hamdani, W. Mahmoud, Synthesis, Characterization and Thermal Study of Some New Metal Ions Complexes with a New Azo 2-((2-(1H-Indol-2-yl) ethyl) diaziny)-5-aminophenol.621 (2023) 121-131.
- [22] A. Majhool, Y. Saleh, O. Aldulaimi, M. Saeed, H. El-Shehry, Syed Azziz, Synthesis of New Azo Dyes of Uracil via Ecofriendly Method and Evaluation For The Breast, Liver and Lung Cancer Cells In vitro. *Chemical Review and Letters*, 6 (2023) 442-448.
- [23] B. Zmejkowski, N. Pantelić, G. Kaluđerović, Palladium (II) complexes: Structure, development and cytotoxicity from cisplatin analogues to chelating ligands with N stereocenters. *Inorganica Chimica Acta*, 534 (2022) 120797.
- [24] A. Malekhoseini, M. Montazerzohori, R. Naghiha, E. Panahi, S. Joohari, Antimicrobial/antioxidant and cytotoxicity activities of some new mercury (II) complexes. *Chemical Review and Letters*, 6 (2023) 166-182.
- [25] Y. Sahar, H. Mohammed, Synthesis, Characterization of Metal Complexes with Azo Ligand Containing Indole Ring and Study of Palladium Complex Activity Against Leukemia. *Arabian Journal for Science and Engineering*, 48 (2023) 7797-7805.
- [26] A. Saeed, S. AlNeyadi, and I. Abdou, Anticancer activity of novel Schiff bases and azo dyes derived from 3-amino-4-hydroxy-2H-pyrano[3,2-c]quinoline-2,5(6H)-dione. *Heterocycl. Commun.*, 26 (2020) 192–205.
- [27] K. D. Issa, Rostam Rasul Braiem, Green and Highly Efficient Synthetic Approach for the Synthesis of 4-Aminoantipyrine Schiff Bases, *Chem. Rev. Lett.* 6 (2023) 2-6.
- [28] S. S. Othman, M. N. Abdullah, Synthesis of Novel Michael Adducts and Study of their Antioxidant and Antimicrobial Activities, *Chem. Rev. Lett.* 6 (2022) 226-233.
- [29] M. Sheydaei, M. Edraki, Antimicrobial evaluation of *Garcinia cambogia*-impregnated sodium montmorillonite, *Chem. Res. Technol.* 1 (2024) 16-21.
- [30] K. De Haan, Y. Zhang, J. Zuckerman, T. Liu, A. Sisk, M. Diaz, K. Jen, A. Nobori, S. Liou, S. Zhang, R. Riahi, Y. Rivenson, W. Wallace, A. Ozcan, Deep learning-based transformation of Hand E stained tissues into special stains. *Nat. Commun.* 12 (2021) 1-13.
- [31] W. Kzar, H. Mohammed, F. Zghair, Z. Zizi Z , Synthesis, Characterization and Staining Ability of Novel Azo Dye Based on Curcumin and Its Au (III) Complex. *Indonesian Journal of Chemistry*.23 (2023) 1375-1383